Research Article | Vol. 27, No. 16 / 5 August 2019 / Optics Express 22275

Optics EXPRESS

Determining the continuous thermo-optic coefficients of chalcogenide glass thin films in the MIR region using FTIR transmission spectra

YUANRONG FANG,[1] DAVID FURNISS,[1] DINUKA JAYASURIYA,[1,2] HARRIET PARNELL,[1,3] ZHUOQI TANG,[1] ANGELA B SEDDON,[1] AND TREVOR M BENSON[1,*]

[1] *Mid-Infrared Photonics Group, George Green Institute for Electromagnetics Research, Faculty of Engineering, University of Nottingham, University Park, NG7 2RD Nottingham, UK*

[2] *Now at ThorLabs, 1 St. Thomas Place, Ely, CB7 4EX, UK*

[3] *Now at Granta Design Ltd. (Materials Intelligence), Rustat House, 62, Clifton Rd., Cambridge, CB1 7EG, UK*

[*] *Trevor.Benson@nottingham.ac.uk*

Abstract: A new method (FTIR continuous dn / dT method, n is refractive index and T temperature) for measuring the continuous thermo-optic coefficients of thin transparent films in the mid-infrared (MIR) spectral region is introduced. The technique is based on Fourier transform infrared (FTIR) transmission spectra measured at different temperatures. It is shown that this method can successfully determine the thermo-optic coefficient of chalcogenide glass thin films (of batch compositions $Ge_{20}Sb_{10}Se_{70}$ at. % (atomic %) and $Ge_{16}As_{24}Se_{15.5}Te_{44.5}$ at. %) over the wavelength range from 2 to 25 µm. The measurement precision error is less than ± 11.5 ppm / °C over the wavelength range from 6 to 20 µm. The precision is much better than that provided by the prism minimum deviation method or an improved Swanepoel method.

1. Introduction

Chalcogenide glasses, based on one or more Group 16 elements of the Periodic Table, sulfur (S), selenium (Se), or tellurium (Te), are promising materials for mid-infrared (MIR) applications [1–4]. With additions of germanium (Ge), arsenic (As) or antimony (Sb), the stability and the robustness of chalcogenide glasses can be increased [5,6]. The properties of a wide range of stable glass compositions, MIR transparency, high refractive index, low phonon energy, and high optical non-linearity, make chalcogenide glasses attractive for use in planar photonic integrated circuits [7,8], fiber-based components for supercontinuum generation [9], optical amplification [10–12], and infrared (IR) thermal lenses [13,14] operating in the MIR region. Although many studies have focused on the physical and optical characterization of chalcogenide glasses, the thermo-optic coefficient (variation in the refractive index n of a chalcogenide glass with a change in the temperature T, *i.e.* dn / dT) is an important parameter in, for example, the design of thermal lenses and high-quality photonic devices that is reported infrequently [15–19].

The refractive index change of a chalcogenide glass with temperature is attributed to the thermal excitation of phonons (and electrons in some cases), and can be either positive or negative in sign depending on the composition of the glass. In [15], the thermo-optic coefficients of seventeen glasses in the Ge-As-Se glass system were measured at a wavelength of 4.515 µm by means of a prism coupler with an error of ± 11.2 ppm / °C. A simplified thermal version of the Lorentz-Lorenz formula was used to describe the thermo-optic coefficients of the glasses, indicating that the thermo-optic coefficient was related to the thermal polarizability coefficient

#364704 https://doi.org/10.1364/OE.27.022275
Journal © 2019 Received 9 Apr 2019; revised 8 Jun 2019; accepted 14 Jun 2019; published 23 Jul 2019

Optics EXPRESS

and the thermal expansion coefficient. Wang *et al.* continued the dn / dT study of Ge-As-Se glass system later [16]. The thermo-optic coefficients of $Ge_{14}As_xSe_{86-x}$ at. % (atomic %) and $Ge_xAs_{12}Se_{88-x}$ at. % at a wavelength of 10 µm were presented using spectroscopic ellipsometry with an error of ± 6 ppm / °C. However, the accuracy in measuring the refractive index by means of spectroscopic ellipsometry is inherently limited by surface effects [20] as a thin contamination layer, oxide layer, or small defects on the surface, can all potentially yield different optical constants for the glass. Apart from spectroscopic ellipsometry, the continuous refractive index over the whole MIR region can also be determined by an improved Swanepoel method [21]. This method can determine the refractive index with a standard deviation of precision less than 0.002, which will lead to a maximum error of 75.5 ppm / °C in determining the dn/dT when the measurement temperature range is 53 °C. Therefore, a more accurate method to obtain the continuous dn / dT data of a thin film is highly desired.

In this paper, we propose such a method based on the FTIR transmission spectra at different temperatures to obtain the continuous thermo-optic coefficient of a MIR transparent thin film over the wavelength range from 2 to 25 µm, which is christened as the FTIR continuous dn / dT method. In order to investigate the errors of this method, two hot-pressed chalcogenide glass thin films, one (nominally batched composition $Ge_{16}As_{24}Se_{15.5}Te_{44.5}$ at. %) with a high thermo-optic coefficient, dn / dT, and the other (nominally batched composition $Ge_{20}Sb_{10}Se_{70}$ at. %) with a low dn / dT, that were annealed prior to measurement, were used. Results show that the proposed method can successfully determine the thermo-optic coefficients of the chalcogenide glass thin films over the wavelength range from 6 to 20 µm with a measurement precision error of less than ± 11.5 ppm / °C. Compared to the minimum deviation method and the improved Swanepoel method, the FTIR continuous dn / dT method is shown to provide an improved measurement precision.

2. Basic theory of the FTIR continuous dn / dT method

For normal incidence on an optical thin film with thickness of d, the wavelengths of the transmission extrema can be expressed by [22]:

$$2nd = m\lambda \tag{1}$$

where λ is the wavelength at the maxima or minima of the normal incidence transmission spectrum, n is the refractive index at a wavelength of λ and m is the order number of the extrema, which has integer values for the maxima and half-integer values for the minima. When the thin film is cooled down to a lower temperature T_l, Eq. (1) becomes:

$$n_l = \frac{m\lambda_l}{2d_l} \tag{2}$$

where λ_l is the wavelength at the maxima or minima of the same order m in the normal incidence transmission spectrum at a temperature T_l, d_l is the thickness of the thin film at a temperature of T_l and n_l is the refractive index of the thin film at a wavelength of λ_l. As discussed in our previous work [21], the values of d_l can be determined to a standard deviation of precision of ≤ 0.02 µm by changing the dispersive model of refractive index from a Cauchy model [22] to a two-term Sellmeier model.

When the thin film is heated up to a higher temperature T_h, the thickness d_h of the thin film at a temperature T_h will be calculated by:

$$d_h = d_l(1 + TEC \times (T_h - T_l)) \tag{3}$$

where TEC is defined as the thermal expansion coefficient, which can be determined by means of thermal mechanical analysis (TMA) [23]). With d_h known and the normal incidence of

Optics EXPRESS

transmission spectrum for the thin film at a temperature of T_h obtained, the refractive index for the thin film at T_h is given as:

$$n_h = \frac{m\lambda_h}{2d_h} \tag{4}$$

where λ_h is the wavelength at the maxima or minima of the same order m in the normal incidence transmission spectrum at a temperature of T_h and n_h is the refractive index at a wavelength of λ_h. The wavelengths λ_l and λ_h, which appear in Eqs. (2) and (4), are not the same, so a dispersive model is introduced.

According to [24], a two-dispersive-term Sellmeier model was effective to describe the refractive index dispersion of a chalcogenide glass in the MIR region; this was later confirmed by us in [21]. The two-term Sellmeier mode is given as:

$$n^2 = A + \frac{B_1\lambda^2}{\lambda^2 - {C_1}^2} + \frac{B_2\lambda^2}{\lambda^2 - {C_2}^2} \tag{5}$$

where A, B_1 and B_2 are dimensionless coefficients. C_1 and C_2 indicate the two resonant absorption wavelengths assumed in the model. Two-term Sellmeier fits are then applied to the refractive index data obtained from Eqs. (2) and (4). The thermo-optic coefficient (dn / dT) of the thin film over the temperature range T_l to T_h can now be determined as:

$$\frac{dn(\lambda)}{dT} = \frac{Sellmeierfit(n_h(\lambda) - Sellmeierfit(n_l(\lambda)}{T_h - T_l} \tag{6}$$

A linear variation of dn / dT has been assumed, as used by [15,16] in the temperature range from 20 °C to 100 °C and in the transparent region away from absorption edges.

3. Sample preparation and experimental

3.1. Chalcogenide glass thin film preparation

For preparing the $Ge_{20}Sb_{10}Se_{70}$ at. % and $Ge_{16}As_{24}Se_{15.5}Te_{44.5}$ at. % glass compositions reported in this paper, the Sb (6N purity, Cerac), As (7N purity, Furakawa Denshi) and Se (5N purity, Materion) elemental precursors were purified *via* a vacuum bake-out procedure in order to drive off the more volatile oxides. Ge (5N purity, Materion) and Te (5N purity, Materion) were added to the glass batch untreated. The elements were batched under a nitrogen atmosphere in an MBraun glove-box (≤ 0.1 ppm H_2O and ≤ 0.1 ppm O_2) into a prepared silica glass ampoule (Multi-Lab Ltd, UK, 6 h air-bake followed by 6 h vacuum-bake at ~10^{-3} Pa). After batching, the silica glass ampoule was sealed (under ~10^{-3} Pa vacuum) and placed in a rocking resistance furnace to melt and homogenize the batch, at ~ 850 °C / 12 h for the $Ge_{16}As_{24}Se_{15.5}Te_{44.5}$ at. % composition and at ~ 900 °C / 24 h for the $Ge_{20}Sb_{10}Se_{70}$ at. % composition. The melts were quenched and annealed for 1 h at their on-set T_g (glass transition temperature) before slowly cooling them down to room temperature. This produced glass rods which were ~ 10 mm in diameter and ~ 70 mm in length and which were suitable as fiber-optic preforms.

A hot-pressing technique was developed to prepare thin films of chalcogenide glass; this involved the hot-pressing under vacuum of *circa* 20 mm lengths of fiber, with a nominal diameter of 250 µm, using the home-built hot-press previously described in [21]. The as-annealed preforms (~10 mm diameter and ~ 70 mm length) of $Ge_{20}Sb_{10}Se_{70}$ at. % and $Ge_{16}As_{24}Se_{15.5}Te_{44.5}$ at. % were drawn into unstructured optical fibers using a customized Heathway draw-tower in a 10,000- Class clean-room. The fibers were drawn under a N_2 flow (BOC white-spot) at a glass melt viscosity of around $10^{4.5}$ Pa.s. The final fiber diameter was 250 ± 10 µm. The outer surface of the fibers was shiny and no defects could be seen by naked eye. The actual compositions of the pressed fibers, measured using SEM-EDX, were found to be close to, but slightly different from, the nominal batched compositions ($Ge_{15.1}As_{27.2}Se_{15.2}Te_{42.5}$ at. % and

Optics EXPRESS

$Ge_{21.1}Sb_{10.6}Se_{68..3} \pm 0.5$ at. %.); nominal compositions are used in the subsequent descriptions. Five $Ge_{16}As_{24}Se_{15.5}Te_{44.5}$ at. % fibers, each of about 20 mm length and 250 µm diameter, were cleaved from the $Ge_{16}As_{24}Se_{15.5}Te_{44.5}$ at. % fiber. The five 20 mm lengths of chalcogenide glass fiber were each immersed in propylamine (Sigma-Aldrich 99 mol.%) for 30 min at room temperature under atmospheric pressure. A silica glass ampoule (Multi-Lab Ltd, UK) was used as the container for the propylamine-etching; this was rinsed with distilled water and dried under vacuum ($\sim 10^{-3}$ Pa) prior to use. Subsequently the etched fibers were taken out of the propylamine and were immersed in acetone (99.8%, Sigma Aldrich) for 10 minutes and then each fiber was individually cleaned carefully using isopropanol (IPA, HPLC grade, Fisher Chemical) with optical lens tissue and dried under vacuum ($\sim 10^2$ Pa). The five propylamine-etched, rinsed and dried 20 mm long fibers were then placed on a tungsten carbide (WC) flat plate (800 mm diameter, of flatness 0.08 µm and of surface finish 0.009 µm) and were surrounded by a 25 µm thick stainless-steel shim (Supplier: Hollinbrow Ltd, UK) and then covered by a second WC plate. The fiber samples were hot-pressed under vacuum (10^{-4} Pa) at T_g+ 40 °C (viscosity $\sim 10^8$ Pa s), with a maximum pressure of 700 N between the two WC plates, applied through the top plate. After pressing, the chalcogenide glass samples were cooled to, and annealed at, the onset-T_g (175 °C, according to differential thermal calorimetry, first heating the sample to just above T_g at 10 °C / min, then cooling at 10 °C / min to ambient and then reheating at 10 °C / min to perform the T_g measurement) and then allowed to cool with the WC discs. In order not to damage the samples while opening the press, solvents (acetone and, if necessary, IPA) were squirted into the gap between the two WC carbide plates. $Ge_{20}Sb_{10}Se_{70}$ at. % thin films, this time with a 30 µm target (shim) thickness, were also prepared following the same method. We believe that the hot press step does not introduce elemental loss. No visible loss of material and no volatilized deposits were observed after the pressing process. SEM-EDX analysis of the GeSbSe sample confirmed that the composition of the resulting thin film was unchanged from that of the fiber from which it was pressed to within experimental measurement error.

3.2. Experimental

A Globar™ source, KBr beam splitter and DLaTGSD301 detector were set up in a Fourier transform infrared (FTIR) spectrometer (Bruker IFS 66v/s) to measure the transmission spectra of the hot-pressed thin films (Sect. 3.1) in the wavelength range from 1 to 25 µm; 25 µm was the maximum wavelength possible with this set-up in the Bruker FTIR spectrometer. Due to the low efficiency of the KBr beam splitter and the DLaTGSD301 detector at wavelengths < 2 µm, clear extrema in the transmission spectra were only obtained over the wavelength range from 2 to 25 µm. The chalcogenide glass thin film sample was mounted on a temperature-controlled holder, constructed in-house. The holder with the thin film sample was connected to a rotation stage, constructed in-house, which was accurate up to 0.1 °, installed in the sample compartment of the Bruker 66v/s FTIR spectrometer. In the FTIR spectrometer a He-Ne beam, which was used for FTIR internal-alignment, indicated the position of the Globar™. Careful alignment was undertaken to ensure that the axis of rotation went through the surface of the thin chalcogenide glass film at the focal point of the He-Ne beam and that no lateral displacement of the light took place during rotation. When measuring the transmission spectra of the thin film at a lower temperature, the temperature of the holder was set to be 20 °C. After the holder reached the set temperature, the thin-film sample was left for 20 minutes to obtain a stable temperature. The actual temperature of the sample was measured to be 21.6 ± 0.1 °C using a K-type adhesive thermocouple. Before recording the transmission spectrum of the thin film, a 15-min dry-air and CO_2-removal purging was allowed to minimize the effect of air absorptions. After obtaining the transmission spectrum at normal incidence, the rotation stage was rotated by an angle of 30 ° to obtain the transmission spectrum with an incident angle of 30 °. Then the rotation stage was rotated back to the normal incident position, and was rotated by an angle of 30 ° in the

Optics EXPRESS

other direction. The transmission spectrum with an incident angle of -30 ° was obtained using FTIR spectroscopy. The temperature-controlled holder was later heated up to a set temperature of 80 °C and the temperature of the sample was measured to be 74.6 ± 0.2 °C. The modified transmission spectra were obtained as described above.

For comparison purposes, the (d*n* / dT)s of the $Ge_{16}As_{24}Se_{15.5}Te_{44.5}$ at. % and $Ge_{20}Sb_{10}Se_{70}$ at. % prisms are presented in this paper. The manufacturing procedure of the chalcogenide glass prisms is described in [25]. The temperature of a prism was controlled using the same temperature-controlled holder as used for the thin-film measurements. The temperature of the holder was set to be 15, 40, 60 and 80 °C, respectively. Every time the holder reached the set temperature, a 20-minute dwell was allowed to obtain a stable prism temperature. The actual temperature of the $Ge_{16}As_{24}Se_{15.5}Te_{44.5}$ at. % prism was 15.7 ± 0.1, 36.9 ± 0.1, 53.9 ± 0.2 and 71.1 ± 0.2 °C, respectively. The actual temperature of the $Ge_{20}Sb_{10}Se_{70}$ at. % prism was 15.7 ± 0.1, 37.1 ± 0.1, 54.3 ± 0.2 and 71.4 ± 0.2 °C, respectively. Refractive index measurements at different sample temperatures were carried out using the minimum deviation method [25]. The source used for the prism deviation method was a 3.1 μm interband cascade laser (ICL) fabricated at the Naval Research Laboratory (NRL), USA, (which emitted > 200 mW at 25 °C) [26]. A linear fit was applied to the refractive index data points at different temperatures and the d*n* / d*T* was obtained from the slope of the fit.

The thermal expansion coefficients (TECs) of the $Ge_{16}As_{24}Se_{15.5}Te_{44.5}$ at. % and $Ge_{20}Sb_{10}Se_{70}$ at. % glass compositions were measured using Thermal Mechanical Analysis (TMA) [23]. Figures 1(a) and 1(b) show the TEC *versus* temperature curves over the temperature range from 40 to 100 °C for $Ge_{16}As_{24}Se_{15.5}Te_{44.5}$ at. % and $Ge_{20}Sb_{10}Se_{70}$ at. % glass samples, respectively. A linear fit was applied to both curves in Figs. 1(a) and 1(b), yielding a R^2 (coefficient of determination) of 1; this means the TEC curves were considered to be linear over the temperature range from 40 to 100 °C. The TEC was calculated from the gradient of the curve between 40 and 100 °C, yielding 16.6 ± 0.5 ppm / °C for $Ge_{16}As_{24}Se_{15.5}Te_{44.5}$ at. % and 19.5 ± 0.5 ppm/ °C for $Ge_{20}Sb_{10}Se_{70}$ at. %.

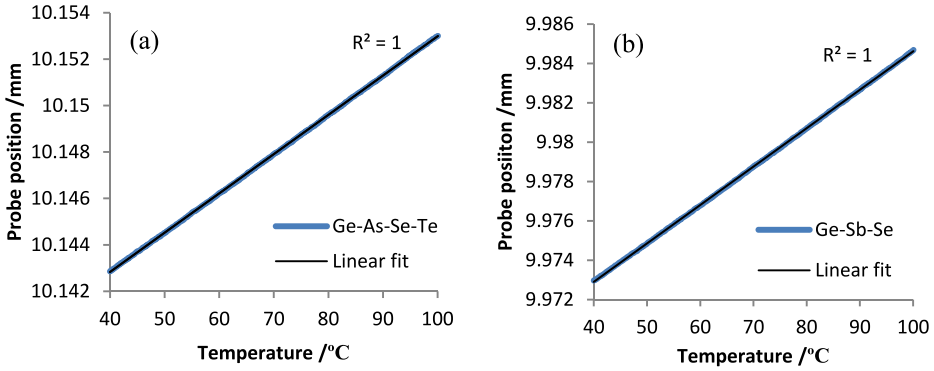

Fig. 1. The thermal expansion coefficient (TEC) curves over the temperature range from 40 to 100 °C for (a) $Ge_{16}As_{24}Se_{15.5}Te_{44.5}$ at. % (Ge-As-Se-Te) and (b) $Ge_{20}Sb_{10}Se_{70}$ at. % (Ge-Sb-Se). Linear fits (R^2 =1) were performed to obtain the values of the TEC for both glasses.

Optics EXPRESS

4. Results and discussion

4.1. *Determining the thermo-optic coefficient of the $Ge_{20}Sb_{10}Se_{70}$ at. % and $Ge_{16}As_{24}Se_{15.5}Te_{44.5}$ at. % thin films*

The transmission spectra of the $Ge_{20}Sb_{10}Se_{70}$ at. % (i.e. Ge-Sb-Se) and $Ge_{16}As_{24}Se_{15.5}Te_{44.5}$ at. % (i.e. Ge-As-Se-Te) thin films at normal incidence at measured temperatures of 21.6 °C and 74.6 °C are shown in Figs. 2(a) and 2(b). The absolute transmittance values shown for Ge-Sb-Se and Ge-As-Se-Te in Figs. 2(a) and 2(b) are not directly comparable as different FTIR beam apertures were used to ensure the beam traveled entirely through each sample.

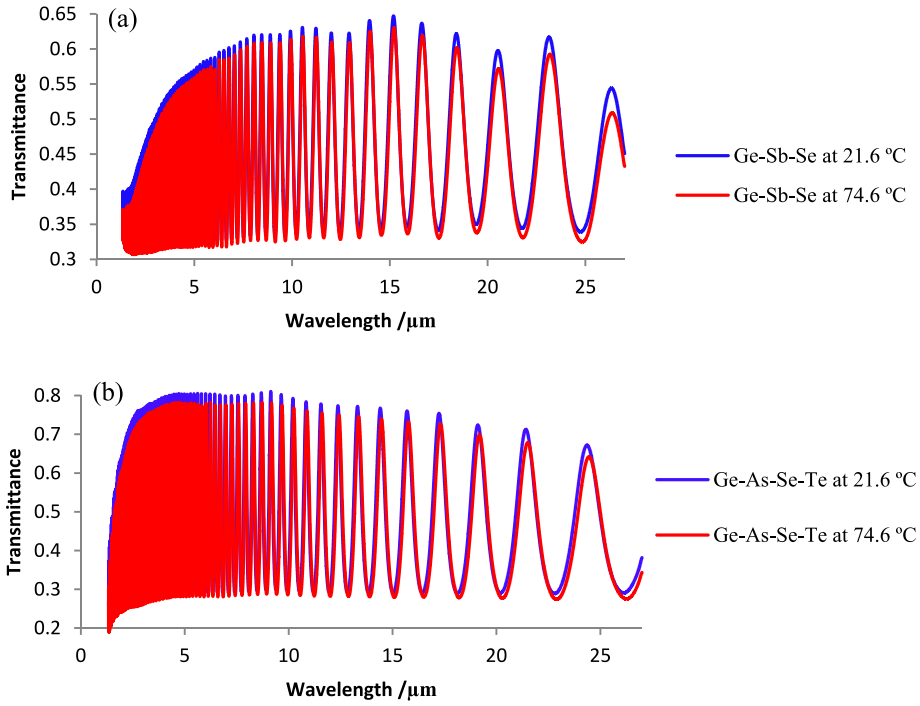

Fig. 2. The transmission spectra were obtained by means of FTIR spectroscopy at normal incidence of: (a) the $Ge_{20}Sb_{10}Se_{70}$ at. % (Ge-Sb-Se) and (b) $Ge_{16}As_{24}Se_{15.5}Te_{44.5}$ at. % (Ge-As-Se-Te) chalcogenide glass thin films, each measured at both temperatures of 21.6 °C and 74.6 °C.

In order to obtain thin film thickness at the lower temperature, the improved Swanepoel method [21] was applied to determine the thickness of the Ge-Sb-Se thin film and of the Ge-As-Se-Te thin film at the lower temperature yielding $d_l = 33.41$ µm and $d_l = 27.40$ µm, respectively. The thickness can be determined to a standard deviation of precision of better than 0.02 µm according to [21]. To obtain the thickness at the higher temperature, the FTIR continuous dn / dT method and the improved Swanepoel method can be applied. For FTIR continuous dn / dT method, the TECs of Ge-Sb-Se and Ge-As-Se-Te were determined by TMA to be 22.4 ppm / °C and 16.6 ppm / °C within the temperature range from 40 to 100 °C, respectively, with an error of ± 0.5 ppm / °C. In the temperature range from 21.6 to 74.6 °C, the TECs of Ge-Sb-Se and Ge-As-Se-Te were assumed to be the same as those obtained within the temperature range from 40 to 100 °C. The thickness of the Ge-Sb-Se and Ge-As-Se-Te thin films at the temperature of 74.6 °C can be determined using Eq. (3), yielding $d_h = 33.445$ µm and $d_h = 27.426$ µm, respectively. For comparison, the improved Swanepoel method was applied to obtain the thickness of the Ge-Sb-Se and Ge-As-Se-Te thin films at the temperature of 74.6 °C directly, yielding $d_l = 33.45$ µm and

Optics EXPRESS

$d_l = 27.43$ µm, respectively. The calculated TECs from the improved Swanepoel method were 22.6 ppm / °C for Ge-Sb-Se and 20.7 ppm / °C for Ge-As-Se-Te. The errors in comparison to the results obtained from TMA are 15.9% and 24.7%. Since the improved Swanepoel can only determine the thickness with a standard deviation of precision of < 0.02 µm, it is not possible to determine the TEC to a high accuracy using this approach.

The order numbers of each extremum in Figs. 2(a) and 2(b) were determined as described in [21]. With m, d_l and d_h of the Ge-Sb-Se and Ge-As-Se-Te thin films obtained, the refractive index data points of Ge-Sb-Se and Ge-As-Se-Te at temperatures of 21.6 °C and 74.6 °C could be determined according to Eq. (1), as shown in Figs. 3(a) and 3(b). The respective two-term Sellmeier fits applied to the data points are shown in Fig. 3, and the Sellmeier coefficients for the best fits are shown in Table 1. The R^2 coefficient of determination in Table 1 is a statistical measure of how well the refractive index model fits the data points. An R^2 of 1 indicates that the refractive index model perfectly fit the data, and here ranges from 0.9996 to 0.9999.

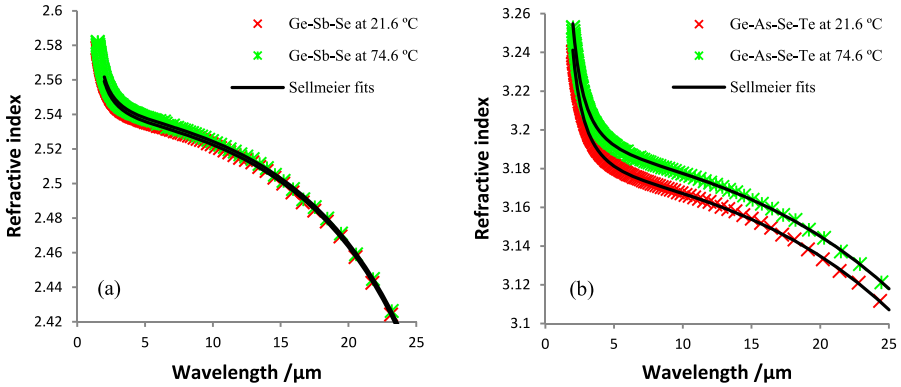

Fig. 3. The refractive indices at different temperatures obtained using the method proposed in this paper for: (a) $Ge_{20}Sb_{10}Se_{70}$ at. % (Ge-Sb-Se) and (b) $Ge_{16}As_{24}Se_{15.5}Te_{44.5}$ at. % (Ge-As-Se-Te), together with the best Sellmeier fits whose coefficients are shown in Table 1.

Table 1. Sellmeier coefficients for $Ge_{20}Sb_{10}Se_{70}$ at. % (Ge-Sb-Se) and $Ge_{16}As_{24}Se_{15.5}Te_{44.5}$ at. % (Ge-As-Se-Te) thin films from the FTIR continuous dn / dT method described in this paper, and directly using the improved Swanepoel method [21].

Sellmeier coefficients	A	B_1	B_2	C_1	C_2	R^2
Ge-Sb-Se @ 21.6 °C (the FTIR continuous dn/dT method)	3.774	2.655	0.9775	0.4213	38.45	0.9996
Ge-Sb-Se @ 74.6 °C (the FTIR continuous dn/dT method)	3.781	2.658	0.9933	0.4252	38.71	0.9996
Ge-Sb-Se @ 74.6 °C (Improved Swanepoel)	5.034	1.405	1.071	0.5653	39.67	0.9996
Ge-As-Se-Te @ 21.6 °C (the FTIR continuous dn/dT method)	6.603	3.468	1.830	0.6684	57.89	0.9999
Ge-As-Se-Te @ 74.6 °C (the FTIR continuous dn/dT method)	7.159	2.979	2.174	0.7299	62.20	0.9999
Ge-As-Se-Te @ 74.6 °C (Improved Swanepoel)	6.959	3.169	1.964	0.7106	59.59	0.9999

The refractive index dispersion of the Ge-Sb-Se and Ge-As-Se-Te thin films at the temperature of 74.6 °C was also obtained directly from the improved Swanepoel method. For comparison purposes, the Sellmeier coefficients so obtained are shown in Table 1. However, these results are not presented in Fig. 3 as they are indistinguishable from the results of the FTIR continuous dn / dT method with differences in refractive index of only 0.0007 for Ge-Sb-Se and 0.0015 for Ge-As-Se-Te over the wavelength range from 2 to 25 µm.

According to Eq. (6), the thermo-optic coefficients of the Ge-Sb-Se and Ge-As-Se-Te thin films at any wavelength over the wavelength range from 2 to 25 µm can be obtained using the

Optics EXPRESS

Sellmeier coefficients in Table 1. The results obtained from the FTIR continuous dn / dT method are shown as the solid curves in Fig. 4(a) and 4(b), respectively, and the results obtained directly from the improved Swanepoel method are displayed as dash lines.

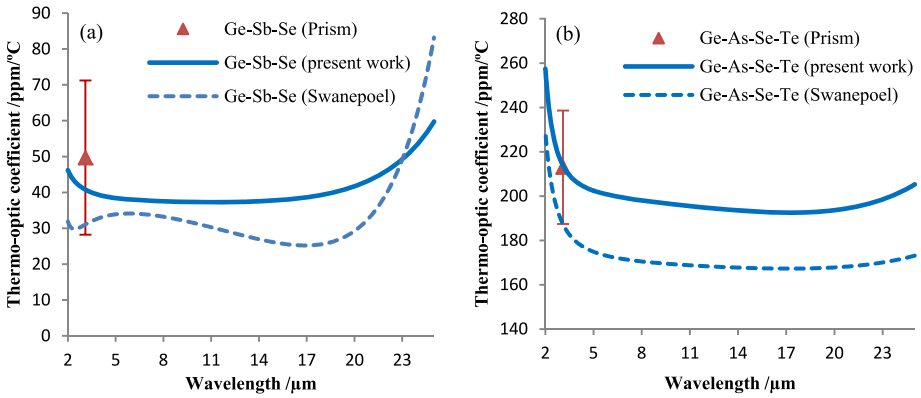

Fig. 4. The thermo-optic coefficient of: (a) $Ge_{20}Sb_{10}Se_{70}$ at. % (Ge-Sb-Se), compared with the results from prism minimum deviation measurements, and (b) $Ge_{16}As_{24}Se_{15.5}Te_{44.5}$ at. % (Ge-As-Se-Te) compared with the results from prism measurement. The thermo-optic coefficients of Ge-Sb-Se and Ge-As-Se-Te obtained directly from the improved Swanepoel method [21] are also displayed as the dashed curves. The measurement precision error of the results obtained from the improved Swanepoel method is ± 75.5 ppm/ °C and is too large to present on the Figures.

4.2. *Error analysis of dn / dT measurements*

The possible sources of errors on the dn / dT measurements using the FTIR continuous dn / dT method are from Δd (error in determining the average thickness at lower temperature d_l), ΔT (thermal stability), ΔTEC (error of the measured thermal expansion coefficient measured using TMA), the error in the Sellmeier fit to refractive index dispersion and the error caused from determining the wavelength of the maxima and minima of the fringes.

According to [21], the improved Swanepoel method can determine the average thickness with a standard deviation of precision of less than 0.02 μm. For the Ge-Sb-Se and Ge-As-Se-Te thin films used in the previous section, this standard deviation error will lead to a low error of less than ±0.02 ppm / °C in calculating the dn / dT, which implies that the FTIR continuous dn / dT method is not sensitive to the average thickness d_l.

In the experiment, the error in measuring the temperature range (dT = T_h - T_l) was < 0.5 °C. A 0.5 °C error in dT will lead to an error of ± 1.5 ppm / °C in determining the dn / dT for the Ge-Sb-Se glass and an error of ± 2.6 ppm / °C in determining the dn / dT for the Ge-As-Se-Te glass. The thermal expansion coefficients were measured by means of TMA to an error of ± 0.5 ppm / °C. This ΔTEC error will result in an error of ± 2.0 ppm / °C in determining dn/dT for Ge-Sb-Se and an error of ± 1.4 ppm / °C in determining dn /dT for Ge-As-Se-Te.

For the two-term Sellmeier fitting, depending on the choice of the resonant wavelengths C_n, several different sets of Sellmeier coefficients can be obtained [22]. Different fits to the same refractive index data points may yield different sets of Sellmeier coefficients with the same R^2. To investigate the error on the dn / dT caused by the different Sellmeier fits, the refractive index at the lower temperature, n_l, and the refractive index at the higher temperature, n_h, of Ge-Sb-Se and Ge-As-Se-Te were each fitted in five different ways to the two-term Sellmeier model. The thermo-optic coefficients of As-Se and Ge-As-Se-Te obtained using these five different sets of Sellmeier coefficients (see Table 2) are shown in Fig. 5. From Fig. 5, it is found that the

Optics EXPRESS

maximum variation in thermo-optic coefficient when using the five different Sellmeier fits is less than ± 3.5 ppm / °C for both Ge-Sb-Se and Ge-As-Se-Te over the wavelength range from 2 to 20 μm. Since few data points are located in the wavelength range from 20 to 25 μm (3 data points for Ge-Sb-Se and Ge-As-Se-Te), and they were affected by strong multi-phonon absorptions, as shown in Fig. 2, the error from the fit to the data points was increased in this longer wavelength range. This leads to a significant error (up to ± 12.5 ppm / °C at a wavelength of 25 μm for Ge-As-Se-Te) in determining the dn / dT within this wavelength region, as shown in Fig. 5.

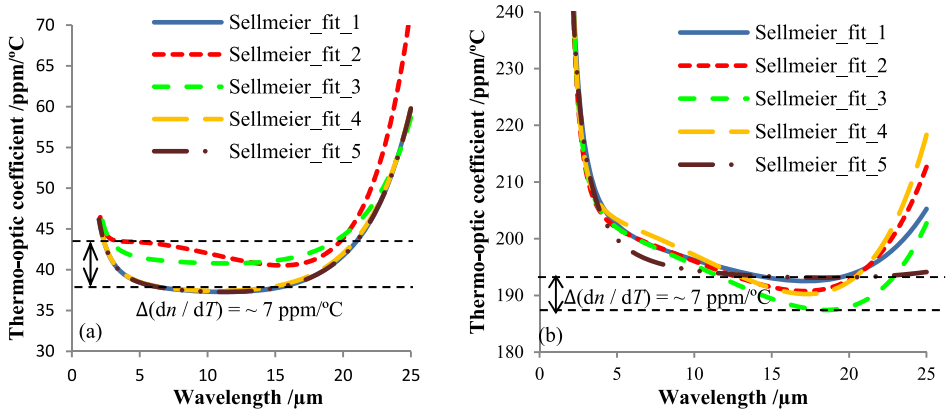

Fig. 5. The thermo-optic coefficients of (a) $Ge_{20}Sb_{10}Se_{70}$ at. % and (b) $Ge_{16}As_{24}Se_{15.5}Te_{44.5}$ at. % obtained using five sets of different Sellmeier fits (shown in Table 2) to the refractive index data points. The envelope of the dotted line shows the maximum variation over the wavelength range from 2 μm to 20 μm.

In the FTIR thin film measurement, the resolution used was 4 cm^{-1}, and the step size of the FTIR spectrum data points was less than 0.4 nm. For Ge-As-Se-Te, this step size will introduce an error of < ± 0.00032 in refractive index at a wavelength of 2 μm, and the error will decrease to < ± 0.00002 in refractive index at wavelengths above 20 μm. Therefore, this will caused an error of 12.0 ppm / °C in dn / dT at a wavelength of 2 μm, and the error will decrease to < ± 1.2 ppm / °C in dn / dT at wavelengths above 20 μm. For Ge-Sb-Se, this step size will introduce an error of < ± 0.00026 in refractive index at a wavelength of 2 μm, and the error will decrease to < ± 0.00002 in refractive index at wavelengths above 20 μm. Therefore, this will caused an error of 9.4 ppm/°C in dn / dT at a wavelength of 2 μm, and the error will decrease to < ± 1 ppm / °C in dn / dT at wavelengths above 20 μm.

To sum up, the error in the dn / dT measurements using the FTIR continuous dn / dT method is mainly attributed to ΔT (thermal stability), ΔTEC (error of the measured thermal expansion coefficient by TMA), the error of the Sellmeier fit and the error caused from determining the wavelengths of the maxima and minima of the fringes. The total error of this technique at the selected wavelengths of 2, 4, 6, 8, 10, 12, 14, 16, 18 and 20 μm is shown in Table 3. When determining the thermo-optic coefficient of low- dn / dT chalcogenide glasses at a wavelength of 2 μm, the error of this technique is less than ± 16.4 ppm / °C, and the error will decrease to ± 7.9 ppm / °C in determining dn / dT at a wavelength of 20 μm, as shown in Table 3. Table 3 also shows that when determining the thermo-optic coefficient of a high- dn / dT chalcogenide glass, the error of this technique is less than ± 19.5 ppm / °C at a wavelength of 2 μm, and decrease to ± 8.7 ppm / °C at a wavelength of 20 μm. At wavelengths below 6 μm, the error will be dominated by the error in determining the absolute wavelengths of maxima and minima of the fringes. At wavelengths above 20 μm, the error will be dominated by the error of the Sellmeier fits. In contrast, the standard deviation of precision in determining the refractive index from the

Optics EXPRESS

Table 2. The different sets of Sellmeier coefficients to the refractive index data points of $Ge_{20}Sb_{10}Se_{70}$ at. % (Ge-Sb-Se) and $Ge_{16}As_{24}Se_{15.5}Te_{44.5}$ at. % (Ge-As-Se-Te).

Sellmeier coefficients	A	B_1	B_2	C_1	C_2	R^2
			Ge-Sb-Se			
Sellmeier 1 @ 21.6 °C	3.774	2.655	0.9775	0.4213	38.45	0.9996
Sellmeier 1 @ 74.6 °C	3.781	2.658	0.9933	0.4252	38.71	0.9996
Sellmeier 2 @ 21.6 °C	3.644	2.784	0.9775	0.4121	38.46	0.9996
Sellmeier 2 @ 74.6 °C	4.440	2.000	1.019	0.4838	39.03	0.9996
Sellmeier 3 @ 21.6 °C	3.848	2.580	0.9920	0.4267	38.65	0.9996
Sellmeier 3 @ 74.6 °C	4.162	2.277	1.006	0.4564	38.87	0.9996
Sellmeier 4 @ 21.6 °C	3.885	2.544	0.9803	0.4297	38.49	0.9996
Sellmeier 4 @ 74.6 °C	3.858	2.581	0.9952	0.4309	38.74	0.9996
Sellmeier 5 @ 21.6 °C	3.740	2.688	0.9766	0.4189	38.44	0.9996
Sellmeier 5 @ 74.6 °C	3.749	2.689	0.9924	0.4229	38.70	0.9996
			Ge-As-Se-Te			
Sellmeier 1 @ 21.6 °C	6.603	3.468	1.830	0.6684	57.89	0.9999
Sellmeier 1 @ 74.6 °C	7.159	2.979	2.174	0.7299	62.20	0.9999
Sellmeier 2 @ 21.6 °C	6.974	3.099	2.041	0.5514	51.53	0.9999
Sellmeier 2 @ 74.6 °C	5.221	4.912	1.448	0.5845	52.72	0.9999
Sellmeier 3 @ 21.6 °C	4.755	5.313	1.372	0.5514	51.53	0.9999
Sellmeier 3 @ 74.6 °C	6.703	3.434	1.865	0.6859	58.35	0.9999
Sellmeier 4 @ 21.6 °C	6.202	3.869	1.737	0.6368	56.73	0.9999
Sellmeier 4 @ 74.6 °C	6.457	3.679	1.762	0.6657	57.0	0.9999
Sellmeier 5 @ 21.6 °C	5.867	4.203	1.644	0.6143	55.56	0.9999
Sellmeier 5 @ 74.6 °C	7.054	3.084	2.138	0.7189	61.79	0.9999

improved Swanepoel method is less than 0.002, which will lead to a ± 75.5 ppm / °C error in the thermo-optic coefficient in the worst case. Therefore, adopting the improved Swanepoel method directly cannot accurately determine the thermo-optic coefficient of chalcogenide glasses. Unlike the improved Swanepoel method, the FTIR continuous dn / dT method is not so sensitive to average thickness and TEC. This is discussed further in the following section.

Table 3. Different sources of errors and the total errors in determining the dn/dT of $Ge_{20}Sb_{10}Se_{70}$ at. % (Ge-Sb-Se) and $Ge_{16}As_{24}Se_{15.5}Te_{44.5}$ at. % (Ge-As-Se-Te) over the wavelength range from 2 to 20 µm.

Wavelength / µm	2	4	6	8	10	12	14	16	18	20
Error (Ge-Sb-Se) / ppm / °C	±16.4	±11.7	±10.1	±9.4	±8.9	±8.6	±8.3	±8.1	±8.0	±7.9
Error (Ge-As-Se-Te) / ppm / °C	±19.5	±13.5	±11.5	±10.5	±9.8	±9.4	±9.2	±9.0	±8.8	±8.7

4.3. Discussion

Figures 2(a) and 2(b) both show that the extrema of the fringes shift to longer wavelengths with increasing temperature. This is consistent with both thermal expansion and a positive thermo-optic coefficient. The shift in wavelength of each extremum observed for Ge-As-Se-Te in Fig. 2(b) is larger than that for Ge-Sb-Se shown in Fig. 2(a). The TEC of Ge-Sb-Se measured using the TMA is larger than that of Ge-As-Se-Te, so this observation is consistent with the larger positive thermo-optic coefficient for Ge-As-Se-Te presented in Fig. 4.

Optics EXPRESS

According to [24], the resonant wavelength C_1 in the two-term Sellmeier model is that wavelength which corresponds to the position of optical band gap of a material and the other resonant wavelength C_2 in the MIR region corresponds to the location of the fundamental vibrational absorption band. The results presented in Table 1 suggest that the resonant wavelengths in the optical band-gap short wavelength region, C_1, and the MIR fundamental vibrational resonant absorption wavelengths, C_2, of Ge-Sb-Se and Ge-As-Se-Te were shifted towards longer wavelengths as the temperature was increased from 21.6 °C to 74.6 °C. This may be summarized as a red shift of the optical bandgap and the fundamental vibrational absorption band with increasing temperature for both the Ge-Sb-Se and Ge-As-Se-Te chalcogenide glasses. In order to confirm red shift of the optical bandgap and the fundamental vibrational absorption band of Ge-Sb-Se and Ge-As-Se-Te, the FTIR absorption spectra for Ge-Sb-Se and Ge-As-Se-Te at temperatures of 21.8 ± 0.2 °C, 37.8 ± 0.2 °C, 55.9 ± 0.3 °C and 74.0 ± 0.3 °C over the wavelength range from 1 to 25 μm were obtained, as shown in Fig. 6(a) and 6(b), respectively. For Ge-Sb-Se, the electronic absorption edge locates at a wavelength < 1 μm (see Fig. 6(a)), but no detailed bandgap information is available. From the inset to Fig. 6(a), the multiphonon absorption band at 17.7 μm was observed to red shift as temperature was increased. For Ge-As-Se-Te, inset (i) to Fig. 6(b) appears to show that the optical band gap shifts to longer wavelengths when increasing the temperature. From inset (ii) to Fig. 6(b), the shoulder at 18.9 μm caused by the multiphonon absorption was observed to shift towards longer wavelengths when increasing the temperature. These observations are in good agreement with the shifts suggested by the resonant wavelengths in the two-term Sellmeier model.

Figure 4 shows that the dn / dT over the temperature range from 21.6 to 74.6 °C of Ge-Sb-Se and Ge-As-Se-Te decreases with increasing wavelength in the shorter wavelength region, which is due to the red shift of the optical band gap with temperature. The dn / dT behavior from 2 to 12 μm is in good agreement with the published dn / dT behavior of Ge-As-Se glasses [16]. At wavelengths > 20 μm, the dn / dT over the temperature range from 21.6 to 74.6 °C starts to increase with wavelength as shown in Fig. 4 This is attributed to the red shift of the fundamental multi-phonon absorption band with temperature as discussed above. For comparison purposes, the thermo-optic coefficients of a $Ge_{20}Sb_{10}Se_{70}$ at. % prism and a $Ge_{16}As_{24}Se_{15.5}Te_{44.5}$ at. % prism measured by us at a wavelength of 3.1 μm are given in Figs. 4(a) and 4(b), with a measurement precision error of < ±21.5 ppm / °C for $Ge_{20}Sb_{10}Se_{70}$ at. % and < ±25.6 ppm / °C for $Ge_{16}As_{24}Se_{15.5}Te_{44.5}$ at. %.

From Fig. 4(a), the difference between the dn / dT of Ge-Sb-Se obtained from the FTIR continuous dn / dT method and that obtained from the prism minimum deviation measurement at a wavelength of 3.1 μm is less than < 9.0 ppm / °C, which is within the error in determining the dn / dT using the minimum deviation method (±21.5 ppm / °C). The thermo-optic coefficient obtained directly from the improved Swanepoel method is also shown as a function of wavelength in Fig. 4(a). The difference between these results and those obtained from the FTIR continuous dn / dT method is less than 13.7 ppm / °C from 2 to 25 μm, which is caused by an extremely small refractive index difference at the temperature of 74.6 °C (0.0007) between the FTIR continuous dn / dT method and the improved Swanepoel method.

From Fig. 4(b), the difference between the dn / dT of Ge-As-Se-Te obtained from the FTIR continuous dn / dT method and that obtained from the prism minimum deviation measurement at a wavelength of 3.1 μm is < 0.7 ppm / °C. The thermo-optic coefficient for Ge-As-Se-Te obtained from the improved Swanepoel method is 25.8 ppm / °C lower than the prism result as shown in Fig. 4(b). In this case, the refractive index difference at the temperature of 74.6 °C between the improved Swanepoel method and the FTIR continuous dn / dT method is less than 0.0015 at the wavelength of 3.1 μm, which leads to a ~28.3 ppm / °C difference in value of the dn / dT.

The error analysis showed that the FTIR continuous dn / dT method could determine the dn / dT of Ge-Sb-Se and Ge-As-Se-Te chalcogenide glasses over the wavelength range from 6 to

Optics EXPRESS

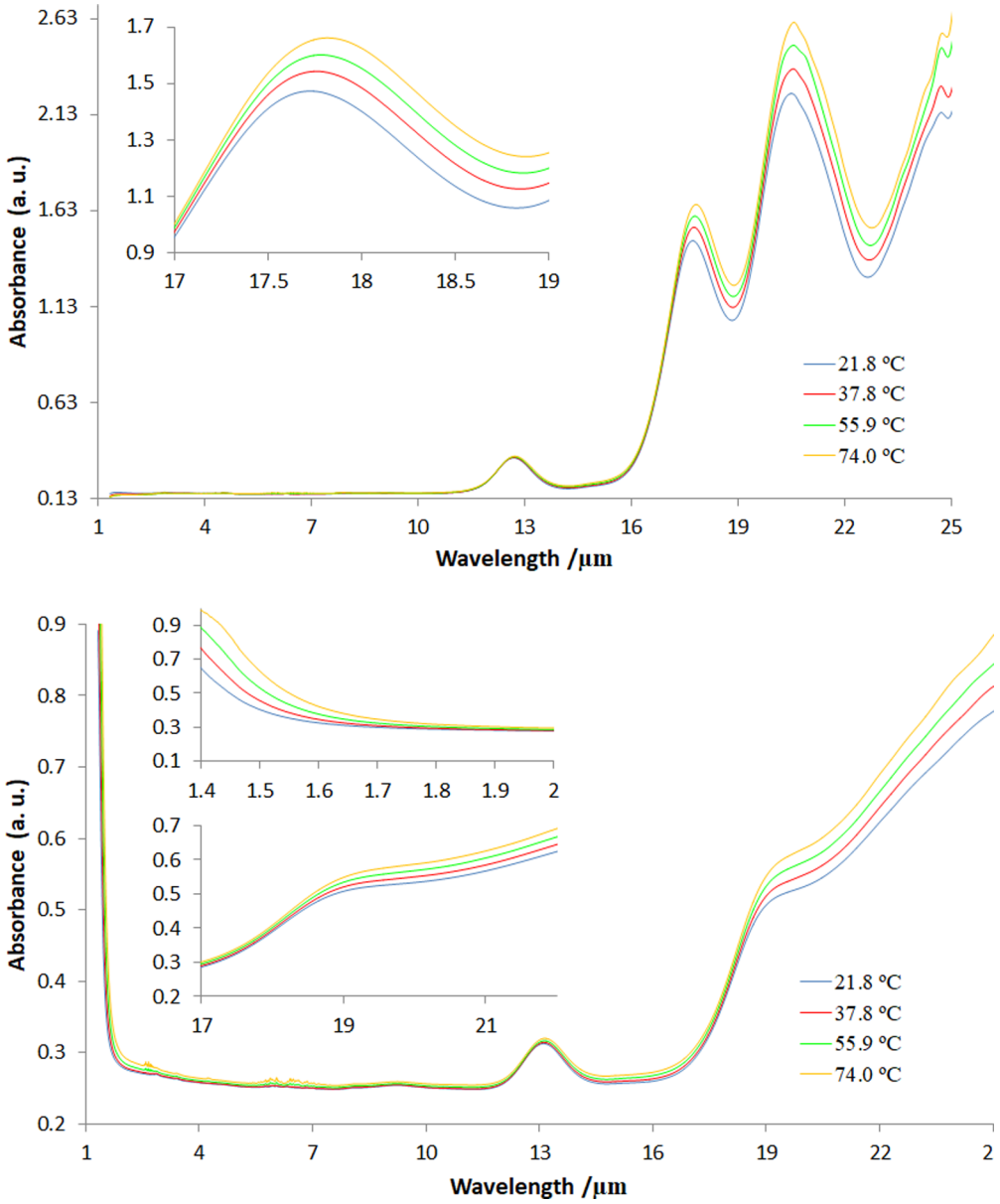

Fig. 6. The FTIR absorbance spectra of (a) a bulk ~ 3 mm optical path-length $Ge_{20}Sb_{10}Se_{70}$ at. % (Ge-Sb-Se) and (b) a bulk ~ 1.5 mm optical path-length $Ge_{16}As_{24}Se_{15.5}Te_{44.5}$ at. % (Ge-As-Se-Te) at temperatures of 21.8 ± 0.2 °C (blue), 37.8 ± 0.2 °C (red), 55.9 ± 0.3 °C (green) and 74.0 ± 0.3 °C (purple) over the wavelength from 1 to 25 µm. Inset to Fig. 6(a) shows the red-shift of the multiphonon absorption at ~ 17.7 µm for Ge-Sb-Se as temperature increased. Inset (i) to Fig. 6(b) shows the red-shift of the optical bandgap for Ge-As-Se-Te as temperature increased and inset (ii) to Fig. 6(b) shows the red-shift of the multiphonon absorption shoulder as temperature increased.

Optics EXPRESS

20 μm and over the temperature range of 21.6 to 74.6 °C with a measurement precision error of less than ± 11.5 ppm/°C. This error is lower than that provided by the prism minimum deviation measurement (±25.6 ppm / °C), the improved Swanepoel method (±75.5 ppm / °C).

5. Conclusions

The continuous thermo-optic coefficients (dn / dT) of the $Ge_{20}Sb_{10}Se_{70}$ at. % and $Ge_{16}As_{24}Se_{15.5}Te_{44.5}$ glass thin films were successfully determined over the wavelength range from 2 to 20 μm and temperature range of 21.6 to 74.6 °C using a new method presented here, named for convenience the FTIR continuous dn / dT method. The error analysis showed that the error of this technique is less than ± 11.5 ppm / °C over the wavelength range from 6 to 20 μm. This technique requires knowledge of the thickness of the thin film, its thermal expansion coefficient, and interference transmission spectra at normal incidence at both a lower temperature and upper temperature; here the temperature difference of these was 53 °C. A two-term Sellmeier model, with one resonant electronic absorption near the optical bandgap and one resonant fundamental vibrational absorption in the mid-infrared, was applied to describe the refractive index dispersion at temperatures of 21.6 and 74.6 °C of the $Ge_{20}Sb_{10}Se_{70}$ at. % and $Ge_{16}As_{24}Se_{15.5}Te_{44.5}$ at. % glass thin films over the wavelength range from 2 μm to 25 μm. The red shifts of the optical bandgap and the fundamental vibrational absorption band with increasing temperature from 21.6 to 74.6 °C were indicated by the values of the resonant wavelengths C_1 and C_2 in the best Sellmeier fit. Compared to the improved Swanepoel method [21], the FTIR continuous dn / dT method was not sensitive to the average thickness of the thin film and thus the error in determining the thermo-optic coefficient is much smaller. Compared to the prism minimum deviation method, the FTIR continuous dn / dT method provides a much lower error and the dn / dT can be easily interpolated at arbitrary wavelengths over the wavelength range from 2 μm to 20 μm. To our best knowledge, it is the first time that the continuous thermo-optic coefficient over this broad MIR region is reported.

Funding

Newton Fund (277109657); Engineering and Physical Sciences Research Council (EPSRC) (EP/P013708/1).

Acknowledgments

The authors acknowledge, with thanks, the partial funding of this work received from a Newton Fund International Links Award (ref. 277109657). We thank Dr J. Meyer of the Naval Research Laboratory for supplying the 3.1 μm ICL (interband cascade laser) used for the prism measurements reported in this work. We are also grateful to the Engineering and Physical Sciences Research Council for their funding of Zhuoqi Tang through the COOL (COld-cOntainer processing for Long-wavelength mid-infrared fibreoptics) project [grant number EP/P013708/1].

References

1. J. S. Sanghera and I. D. Aggarwal, "Active and passive chalcogenide glass optical fibers for IR applications: a review," J. Non-Cryst. Solids **256-257**(2), 6–16 (1999).
2. J. S. Sanghera, L. B. Shaw, and I. D. Aggarwal, "Chalcogenide glass-fiber-based mid-IR sources and applications," IEEE J. Sel. Top. Quantum Electron. **15**(1), 114–119 (2009).
3. A. B. Seddon, "Chalcogenide glasses: a review of their preparation, properties and applications," J. Non-Cryst. Solids **184**(1), 44–50 (1995).
4. B. Eggleton, B. Luther-Davies, and K. Richardson, "Chalcogenide photonics," Nat. Photonics **5**(3), 141–148 (2011).
5. D. Lezal, "Chalcogenide glasses-survey and progress," J. Optoelectron. Adv. Mater. **5**(1), 23–34 (2003).
6. A. Zakery and S. R. Elliott, "Optical properties and applications of chalcogenide glasses: a review," J. Non-Cryst. Solids **330**(1-3), 1–12 (2003).

Optics EXPRESS

7. A. B. Seddon, W. J. Pan, D. Furniss, C. A. Miller, H. Rowe, D. M. Zhang, E. M. McBrearty, Y. Zhang, A. Loni, P. Sewell, and T. M. Benson, "Fine embossing of chalcogenide glasses – a new fabrication route for photonic integrated circuits," J. Non-Cryst. Solids **352**(23-25), 2515–2520 (2006).
8. N. S. Abdel-Moneim, C. J. Mellor, T. M. Benson, D. Furniss, and A. B. Seddon, "Fabrication of stable, low loss optical loss rib-waveguides via embossing of sputtered chalcogenide glass-film on glass-chip," Opt. Quantum Electron. **47**(2), 351–361 (2015).
9. C. R. Petersen, U. Møller, I. Kubat, B. Zhou, S. Dupont, J. Ramsay, T. Benson, S. Sujecki, N. Abdel-Moneim, Z. Tang, D. Furniss, A. B. Seddon, and O. Band, "Mid-infrared supercontinuum covering the 1.4-13.3 mum molecular fingerprint region using ultra-high NA chalcogenide step-index fibre," Nat. Photonics **8**(11), 830–834 (2014).
10. J. Hu, C. R. Menyuk, C. Wei, L. B. Shaw, J. S. Sanghera, and I. D. Aggarwal, "Highly efficient cascaded amplification using Pr^{3+}- doped mid-infrared chalcogenide fiber amplifiers," Opt. Lett. **40**(16), 3687–3690 (2015).
11. M. C. Falconi, G. Palma, F. Starecki, V. Nazabal, J. Troles, J. Adam, S. Taccheo, M. Ferrari, and F. Prudenzano, "Dysprosium-doped chalcogenide master oscillator power amplifier (MOPA) for mid-IR Emission," J. Lightwave Technol. **35**(2), 265–273 (2017).
12. M. Shen, D. Furniss, Z. Tang, E. Barny, L. Sojka, S. Sujecki, T. M. Benson, and A. B. Seddon, "Modeling of resonantly pumped mid-infrared Pr^{3+}-doped chalcogenide fiber amplifier with different pumping schemes," Opt. Express **26**(18), 23641–23660 (2018).
13. X. H. Zhang, Y. Guimond, and Y. Bellec, "Production of complex chalcogenide glass optics by molding for thermal imaging," J. Non-Cryst. Solids **326-327**, 519–523 (2003).
14. D. Cha, H. Kim, Y. Hwang, J. Jeong, and J. Kim, "Fabrication of molded chalcogenide-glass lens for thermal imaging applications," Appl. Opt. **51**(23), 5649–5656 (2012).
15. B. Gleason, K. Richardson, L. Sisken, and C. Smith, "Refractive index and thermo-optic coefficients of Ge-As-Se chalcogenide glasses," Int. J. Appl. Glass Sci. **7**(3), 374–383 (2016).
16. Y. Wang, S. Qi, Z. Yang, R. Wang, A. Yang, and P. Lucas, "Composition dependences of refractive index and thermo-optic coefficient in Ge-As-Se chalcogenide glasses," J. Non-Cryst. Solids **459**, 88–93 (2017).
17. J. D. Musgraves, S. Danto, and K. Richardson, "Thermal properties of chalcogenide glasses," In *Chalcogenide Glasses*, 82–112 (2014).
18. Amorphous Materials Inc, "AMTIR-2 Information" (consulted December 2018).
19. Schott Glass Inc, "Schott infrared chalcogenide glasses – IRG 6" (2013).
20. D. Poelman and P. Smet, "Methods for the determination of the optical constants of thin films from single transmission measurements: a critical review," J. Phys. D: Appl. Phys. **36**(15), 1850–1857 (2003).
21. Y. Fang, D. Jayasuriya, D. Furniss, Z. Q. Tang, C. Markos, S. Sujecki, A. B. Seddon, and T. M. Benson, "Determining the refractive index dispersion and thickness of hot-pressed chalcogenide thin films from an improved Swanepoel method," Opt. Quantum Electron. **49**(7), 237 (2017).
22. R. Swanepoel, "Determining refractive index and thickness of thin films from wavelength measurements only," J. Opt. Soc. Am. A **2**(8), 1339–1343 (1985).
23. M. D. O'Donnell, D. Furniss, V. K. Tikhomirov, and A. B. Seddon, "Low loss infrared fluorotellurite optical fibre," Phys. Chem. Glasses: Eur. J. Glass Sci. Technol., Part B **47**(2), 121–126 (2006).
24. H. G. Dantanarayana, N. Abdel-Moneim, Z. Tang, L. Sojka, S. Sujecki, D. Furniss, A. B. Seddon, I. Kubat, O. Bang, and T. M. Benson, "Refractive index dispersion of chalcogenide glasses for ultra-high numerical-aperture fiber for mid-infrared supercontinuum generation," Opt. Mater. Express **4**(7), 1444–1455 (2014).
25. V. Q. Nguyen, J. S. Sanghera, F. H. Kung, P. C. Pureza, and I. D. Aggarwal, "Very large temperature-induced absorptive loss in high Te-containing chalcogenide fibers," J. Lightwave Technol. **18**(10), 1395–1401 (2000).
26. M. S. Maklad, R. K. Mohr, R. E. Howard, P. B. Macedo, and C. T. Moynihan, "Multiphonon absorption in As_2S_3-As_2Se_3 glasses," Solid State Commun. **15**(5), 855–858 (1974).